

Journal Pre-proofs

Binder jetting 3D printing of challenging medicines: from low dose tablets to hydrophobic molecules

Marta Kozakiewicz, Karol P. Nartowski, Aleksandra Dominik, Katarzyna Malec, Anna M. Gołkowska, Adrianna Złocińska, Małgorzata Rusińska, Patrycja Szymczyk-Ziółkowska, Grzegorz Ziółkowski, Agata Górniak, Bożena Karolewicz

PII: S0939-6411(21)00274-5
DOI: <https://doi.org/10.1016/j.ejpb.2021.11.001>
Reference: EJPB 13683

To appear in: *European Journal of Pharmaceutics and Biopharmaceutics*

Received Date: 19 July 2021
Revised Date: 3 October 2021
Accepted Date: 8 November 2021

Please cite this article as: M. Kozakiewicz, K.P. Nartowski, A. Dominik, K. Malec, A.M. Gołkowska, A. Złocińska, M. Rusińska, P. Szymczyk-Ziółkowska, G. Ziółkowski, A. Górniak, B. Karolewicz, Binder jetting 3D printing of challenging medicines: from low dose tablets to hydrophobic molecules, *European Journal of Pharmaceutics and Biopharmaceutics* (2021), doi: <https://doi.org/10.1016/j.ejpb.2021.11.001>

This is a PDF file of an article that has undergone enhancements after acceptance, such as the addition of a cover page and metadata, and formatting for readability, but it is not yet the definitive version of record. This version will undergo additional copyediting, typesetting and review before it is published in its final form, but we are providing this version to give early visibility of the article. Please note that, during the production process, errors may be discovered which could affect the content, and all legal disclaimers that apply to the journal pertain.

© 2021 Published by Elsevier B.V.



Original article

Binder jetting 3D printing of challenging medicines: from low dose tablets to hydrophobic molecules

Marta Kozakiewicz^{1‡}, Karol P. Nartowski^{1‡*}, Aleksandra Dominik^{1‡}, Katarzyna Malec¹, Anna M. Golkowska¹, Adrianna Złocińska², Małgorzata Rusińska³, Patrycja Szymczyk-Ziółkowska³, Grzegorz Ziółkowski³, Agata Górniak², Bożena Karolewicz¹

1. Department of Drug Forms Technology, Wrocław Medical University, Borowska 211 A, 50-556 Wrocław, Poland

2. Laboratory of Elemental Analysis and Structural Research, Wrocław Medical University, Borowska 211 A, 50-556 Wrocław, Poland

3. Centre for Advanced Manufacturing Technologies (CAMT/FPC), Wrocław University of Science and Technology, Łukasiewicza 5, 50-371 Wrocław, Poland

‡ These authors contributed equally.

*Corresponding author: Dr hab. Karol P. Nartowski, Department of Drug Forms Technology, Wrocław Medical University, Borowska 211 A, 50-556 Wrocław, Poland,

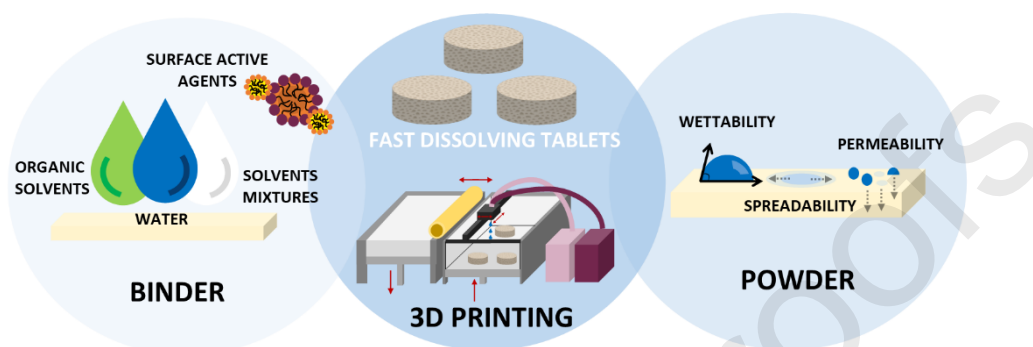
e-mail address: karol.nartowski@umed.wroc.pl

Abstract:

Increasing access to additive manufacturing technologies utilising easily available desktop devices opened novel ways for formulation of personalized medicines. It is, however, challenging to propose a flexible and robust formulation platform which can be used for fabrication of tailored solid dosage forms composed of APIs with different properties (e.g., hydrophobicity) without extensive optimization. This manuscript presents a strategy for formulation of fast dissolving tablets using binder jetting (BJ) technology. The approach is demonstrated using two model APIs: hydrophilic quinapril hydrochloride (QHCl, logP = 1.4) and hydrophobic clotrimazole (CLO, logP = 5.4). The proposed printing method uses inexpensive well known and easily available FDA approved pharmaceutical excipients. The obtained model tablets had uniform content of the drug, excellent mechanical properties and highly porous structure resulting in short disintegration time and fast dissolution rate. The tablets could be scaled and obtained in predesigned shapes and sizes. The proposed method may find its application in the early stages of drug development where high flexibility of the formulation is required and the amount of available API is limited.

KEY WORDS: inkjet printing, 3DP, additive manufacturing, fast dissolving tablets, wettability, clotrimazole, quinapril, spray drying

Graphical abstract (colour print)



The study presents an approach for formulation of 3D printed fast dissolving tablets using binder jetting technology

1. Introduction:

Additive manufacturing (AM) based on Computer Aided Design (CAD) models, commonly recognised as 3D printing (3DP), is rapidly evolving technology that brought new opportunities for the manufacturing of complex and patient tailored medicines [1]. As large-scale pharmaceutical manufacturing cannot fully address the paradigm of personalized medicine due to a lack of flexibility and precision in dosage delivery, AM holds promise in the development of alternative manufacturing protocols. These can potentially be introduced into pharmaceutical practice within pharmaceutical compounding units or hospital pharmacies which meets Good Manufacturing Practice regulations [2–4]. The 2016 has become a landmark year in pharmaceutical industry due to market commercialisation of the first FDA approved 3D printed tablets Spritam® (levetiracetam, BCS class I drug) for treatment of epilepsy. The innovative ZipDose® printing technology developed by Aprelia Pharmaceuticals, Blue Ash OH [5] enabled producing tablets with twice as much API as compared to conventional levetiracetam solid dosage forms and short disintegration time due to their porous structure. While commercial success of the first produced additively tablet confirmed the applicability of this technology in pharmaceutical industry, the high flexibility of this manufacturing technique guarantees further progress in formulation of personalised medicines and novel drug delivery systems.

Within AM technologies applied for manufacturing of novel drug delivery systems various technologies can be named, such as fused deposition modelling (FDM) [6,7], stereolithography (SLA) [8], selective laser sintering (SLS) [9], binder jetting (BJ) [10] and drop-on-demand (DoD) [11,12]. Those

technologies bring wider opportunities for developing tailored drug delivery systems including controlled drug release [13], orally disintegrating tablets [9], solids in various geometrical shapes [6,14,15] and combinations of multiple API with designed drug release profiles [16–18]. This innovative technique is possible, generally due to reversed approach to the additive manufacturing process, where materials are processed and/or joined selectively, forming the final product by building it up. Furthermore, additive manufacturing provides a precise control of the shape, size and distribution of an API in the Drug Delivery Systems (DDSs), therefore, it allows to design the desired release profile of a drug by combining CAD (Computer Aided Design) and knowledge of drug and excipient properties [1,19,20]. While the AM technologies portfolio is continuously growing, some of their representatives has been proved successful in pharmaceutical applications. The Drop-on-Demand (DoD) inkjet printing is of increasing interest as it enables contactless, precise, and reproducible deposition of small volumes (drop-wise) of a liquid (solution/suspension [11,12]) on various substrates from edible paper [21] and polymeric films [22,23] to porous materials [12,24]. Up-to-date inkjet printing has been employed to enhance dissolution of poorly water soluble drugs [4,21,23,25,26], investigate crystallisation outcomes and phase transitions of printed drug molecules [23,27,28] or prepare personalised/paediatric doses of drugs [3,15,24,29]. While inkjet printing on flat or homogenous surfaces has recently gained wider recognition, there are only few reports on binder jetting on powdered material [30]. This technology is based on the selective binder droplets deposition onto a thin layer of powder through position and motion-controlled print-heads, following the given cross-section of the CAD model, enabling to bind powder particles (excipients and/or drug) together (Scheme 1) [30,31]. After the first layer is ‘printed’ the powder bed is lowered, and another thin layer of powder is firmly deposited and the printing process is repeated, until the whole model is finished [30]. The model formulation is based on the binding of powder particles as a reaction to the deposited binder solution, both in one layer and between them. This process was first applied to print fast dissolving tablets of hydrophilic captopril ($\log P = 0.34$) in combination with small content of maltitol, maltodextrin and polyvinyl pyrrolidone [30]. As demonstrated later by Yu et al. [32] using similar fabrication method it was possible to obtain a multi-layered doughnut-shaped DDS wherein acetaminophen, a poorly water-soluble drug, was sandwiched between ethyl cellulose rich, drug-free top and bottom barrier enabling a linear drug release profile. Similarly, Wang et al. [31] presented a 3D printed cubic core-shell DDS with a near zero-order release profile composed of hydrophilic drug pseudoephedrine hydrochloride and a mixture of release modifying polymers Kollidon SR and HPMC. The precise control of shape, size and dose in AM devices was demonstrated in the formulation of controlled-release levofloxacin and rifampicin drug implant with complex architecture [33]. The designed implant consists of the levofloxacin-rich bottom and core-shell top composed of rifampicin (core) coated with L-PLA layer (shell) [33].

Despite several examples presenting the high design flexibility of AM, this modern manufacturing method may face some challenges when it comes to printing large doses of hydrophobic molecules of

poor wettability or the necessity of using water-based binders. For example, the printing quality of poorly water soluble compounds in inkjet printers can be affected by binder spread and its permeation through the powder bed resulting in the displacement of powder layers [20]. As nearly 50% of currently marketed drugs and an estimated 70% of pipeline APIs are poorly water soluble [34] compounds, establishing the robust experimental protocols enabling the 3DP processing of poorly soluble pharmaceuticals is of increasing importance in additive manufacturing technologies. As the drug can either be incorporated in a powder bed and/or dissolved in binder solution different approaches need to be considered. For example, the use of organic solvents as binders is frequently utilised in 3DP of pharmaceuticals as these display both lower viscosity and lower surface tension as compared with water-based binders and can easily solubilise hydrophobic drugs. Furthermore, the addition of surfactants and/or use of mixtures of water with organic solvents can successfully enhance the spreadability and permeation of binders onto the powder bed. However, both protocols create the problem of efficient removal of toxic solvent from the final formulation. An alternative to the use of organic solvents can be the micellar solubilisation approach described by Payumo et al. [35] in their patent. This method involves the mixture of drug and solubilising agent to form micelles that increase the solubility of a compound in water [1]. Regardless of whether the drug is incorporated in the powdered bed or dissolved in the binder solution, it is important to control its crystalline form in the final formulation, as it may affect the dissolution process and, consequently, the bioavailability of the API. Mèlendez et al. [36] described the change in the polymorphic form of prednisolone from I to III after printing using a water/ethanol/glycerol mixture. While recently Kollamaram et al. [23] reported polymorphic selectivity between acetaminophen forms I and II crystallising from the ink on smooth or flat surfaces. Highlighted examples indicate the need for careful selection of both the ink composition as well as the surface properties onto which the binder is deposited to ensure the stability of the drug form in the final product.

The high number of APIs with poor powder properties (e.g., poor flow or compressibility) has led to the search for new methods and excipients to improve them. For example, Erdemir et al. [37] presented the enhancement of bulk density and flow properties through co-precipitation of theophylline crystals with polyvinylpyrrolidone-vinyl acetate (PVPVA). The precipitating polymer formed spherical agglomerates with crystalline API providing enhanced flow and bulk density of the final composite [37]. Vanhoorne et al. [38] and Shi et al. [39] processed paracetamol crystals with amorphous lactose, PVP and HPC to improve its poor compressibility enabling extensive binder-binder contacts. Furthermore, co-processing hydrophobic crystals with amorphous lactose can provide uniform delivery of steroids to the lung as demonstrated in Bay et al. [40] patent. As a part of this study, we developed an approach of embedding hydrophobic crystals within hydrophilic matrices made of PVP or lactose using spray drying. This method enabled us to enhance wettability and binding properties of selected APIs.

This study evaluates the effect of hydrophobic properties of APIs and selected excipients (microcrystalline cellulose, ethyl cellulose, methylcellulose, polyvinylpyrrolidone, hydroxypropyl

methylcellulose) on their printability using binder jetting technology (BJ). To assess the effect of wettability of pharmaceutical substances by binder solutions we tested six excipients and seven APIs in contact with water, water:ethanol mixtures, organic solvents, and their mixtures with surface active agents. Based on the optimization of ink composition and powder bed properties we selected clotrimazole (CLO) as model hydrophobic API to evaluate presented in this work approach of API-excipient co-processing via spray drying and its application to enhance printability of hydrophobic molecules via water-based binders. As a second model quinapril hydrochloride (QHCl) was selected to evaluate printability of hydrophilic molecule mixed with pharmaceutical excipients to obtain small dosage (3 mg) fast dissolving tablets. Selected substances belonged to different classes according to the BCS, differing in their water solubility and penetration through biological membranes. The approach proposed in this work may serve as a good starting point for process and materials optimization for inkjet printing of other APIs with either hydrophilic or hydrophobic properties.

2. Materials and Methods:

2.1 Materials: Quinapril hydrochloride, clotrimazole and lactose monohydrate were donated by P.P.F. “Hasco-Lek” (Wroclaw, Poland). Paracetamol, ibuprofen, naproxen, and famotidine were donated from US Pharmacia Sp. z o.o. (Wroclaw, Poland). Microcrystalline cellulose and polyvinylpyrrolidone-25 (PVP) were donated by Pharmaceutical Research Institute (Warsaw, Poland). Tween 20, ethyl cellulose and flufenamic acid were purchased from Sigma Aldrich (Saint-Luis, MA, USA). Sodium Dodecyl Sulphate (SLS), methylcellulose, hydroxypropyl methylcellulose (HPMC, 4000 and 100000 cps), were purchased from P.P.H. „STANLAB” Sp.J. (Lublin, Poland). Acetonitrile, isopropanol, dichloromethane and HPLC quality water were purchased from T.J. Baker (Deventer, Netherlands). Concentrates of phosphate (pH = 6,8) and acetate (pH = 4.0) buffers as well as 0.1 M hydrochloric acid concentrate for dissolution were purchased from Chemlab Sp. z o.o. (Kielce, Poland). Acetonitrile and methanol for HPLC was purchased from Merck (Darmstadt, Germany).

2.1.1 Formulation of binder solutions: Binder solutions were formulated as follows: PVP was accurately weight (12 or 22 wt./V %) and dissolved in a solvent (water, water/ethanol mixture, methanol, isopropanol, dichloromethane, or acetonitrile), following the addition of Tween 20 and SLS. The binder solution used for BJ process was chosen based on its wetting and powder bed penetration properties. The composition of evaluated binder solutions is given in the ESI, Table S1.

2.1.2 Formulation of powder bed: Several excipients and their mixtures with API were evaluated as components of a powder bed. APIs were formulated as powder blends with microcrystalline cellulose (MC), PVP, methylcellulose, ethyl cellulose or HPMC in different ratios. The powder bed used for 3DP was chosen based on its good wetting

properties, lack of gelation upon binder addition and good penetration of the binder through the powder bed (see section 3 for details).

2.2 Methods:

2.2.1 *Determination of a contact angle for powder bed:* APIs, excipients or mixtures of powders were placed in the 3D printed containers (see ESI, Figure S1) and pressed with metallic block to mimic the conditions during inkjet printing, which resulted in flat and compacted powder surfaces. The contact angle and binder drop permeability through the selected powders was measured using Contact Angle Goniometer (Osilla Ltd., Sheffield, UK) and provided software. Short movies were recorded using high resolution camera at 30 FPS. The wetting angle formed between the solid surface of a powder and the liquid drop surface was measured using the frame of the film at which the drop landed at the powder surface.

2.2.2 *Density measurement:* A pycnometer (Brand, Wertheim, Germany) was used to determine the volumes of binder samples. Water and a mixture of water and ethanol (50/50 V/V) were used as the reference liquid. The mass of the tested sample was determined with an analytical balance (Sartorius, Germany). Density was calculated as the ratio of mass to volume.

2.2.3 *Viscosity measurement:* The falling-ball viscometer (VISCOBALL, Fungilab, Barcelona, Spain) was used to determine the viscosity of the binders by measuring the time the ball falls in the liquid. Calibration of the viscometers was obtained using a reference standard - water and a mixture of water and ethanol (50/50 V/V). The ball falling angle was 80°, the falling was at a thermostatically controlled temperature of 20 °C. The viscosity was calculated using the following equation:

$$\eta_1 = k(\rho_k - \rho_c) \cdot t, \text{ Eq. 1}$$

where $k \left[\frac{\text{mPa} \cdot \text{s} \cdot \text{cm}^3}{\text{g} \cdot \text{s}} \right]$ is ball constant, $\rho_k \left[\text{g} \cdot \text{cm}^3 \right]$ is ball density, $\rho_c \left[\text{g} \cdot \text{cm}^3 \right]$ is product density at measurement temperature and $t \left[\text{s} \right]$ is arithmetic average ($n = 3$) of the falling ball time.

2.2.4 *Surface tension measurement:* The surface tension measurements were performed using a Sigma 703 tensiometer (KSV Instruments LTD, Helsinki, Finland) with a platinum ring of medium circumference 6.28 cm. A 20 mL sample in a beaker was considered sufficient to completely wet the ring. The samples were tested at a constant temperature of 20 °C.

2.2.5 *SEM Imaging:* To evaluate the morphology and grain size of powders as well as the surface and internal structure of manufactured tablets, a field emission scanning electron microscope (Zeiss, Sigma 500 VP) was used. Before the measurements, the samples were covered with gold (sputter current 40 mA, sputter time 50 s) using a Quorum machine (Quorum International, USA) to improve the discharge process.

2.2.6 *CT analysis*: The spatial structure of the tablets was analysed with the XCT technical computed tomography system: GE Phoenix v | tome | x m 300/180 and phoenix datos | x2.7.2 reconstruction software (GE Sensing & Inspection Technologies GmbH, Wunstorf, Germany). Four tablets were selected for the study. A transmission lamp with a nanofocus allowed the reconstruction of tablets with a voltage of 80 kV and an intensity of 300 μ A. Each reconstruction was made based on 3000 projections, with a single projection recording time of 400 ms by the detector. During the test, the distance between the tablets and the lamp (FOD) was 28.37 mm, while the distance between the detector and the lamp (FDD) was 801.61 mm, allowing for a resolution (voxel size) of 7 μ m. The analysis of the data obtained in this way was performed using the VG Studio MAX 3.3 software (Volume Graphics GmbH, Heidelberg, Germany).

2.2.7 *Clotrimazole crystals co-processing using spray drying*: To mask hydrophobic properties of clotrimazole and increase the mechanical properties of obtained tablets the drug crystals were co-processed with hydrophilic compounds PVP or lactose at 75:25; 50:50 and 25:75 drug:excipient ratio (wt./wt.) using spray drying. For example, to synthesise 50:50 CLO:PVP material 2.5 g of CLO was suspended in PVP solution (2.5 g of PVP dissolved in 250 mL of deionised water) resulting in 1% wt./V suspension of CLO crystals in PVP solution. The suspensions were spray dried using a Mini Spray Dryer B-290 (Büchi, Flawil, Switzerland). The feeding suspensions were atomized through a 0.7 mm two-fluid nozzle using dry compressed air at the pressure of 5 bar. The spray drying was carried out under the following conditions: peristaltic pump rate 5.0 mL \cdot min⁻¹, compressed air flow rate 414 L \cdot h⁻¹, aspiration rate 37 m³ \cdot h⁻¹, inlet temperature 160 \pm 2 $^{\circ}$ C and outlet temperature 100 \pm 1 $^{\circ}$ C. The obtained material was separated in a cyclone, collected, and stored in a desiccator over a silica gel until further analysis.

The efficiency of the spray drying (SD_{eff} [%]) was calculated using the following equation (see ESI Table S2):

$$SD_{eff} = \frac{M_p}{M_s} \times 100\%, \text{ Eq. 2}$$

where M_p [g] is the mass of the spray dried product and M_s [g] is the mass of the CLO and PVP (or lactose) used for suspension preparation.

The CLO suspensions in the lactose solutions required the addition of 0.5 mL of Tween 20 prior spray drying to avoid clogging of CLO particles. The 2% w/V CLO suspension in water with 0.5 mL Tween 20 was also spray dried to consider the effect of Tween 20 on powder wettability.

2.2.8 *Tablets printing*: The tablets were obtained using inkjet printer Spectrum Z 510 (Z Corporation, Rock Hill, SC, USA) utilising binder jetting printing technique. The special set of smaller chambers and containers for the overpower drop was used, to minimize the

use of needed material for the process and waste. To provide easy to clean and change, a dedicated binder depositing system was designed and manufactured to replace the original one. Three main process parameters were considered: the thickness of a powder layer was 125 μm and 50% saturation of model cross-section on the powder bed and 2 hours of free evaporation were determined as optimal for tablet formulation. Different geometries were designed and tested, finally, the oval-shaped tables with the preliminary dimensions of 12.5 x 4.5 x 5.5 mm were selected as placebo (Series A) and QHCl (Series B) tablets and scaled to obtain CLO tablets with high API content (Series C and D). To prevent the lower layers of tablets to be deformed while applying subsequent layers, the support structure was added to the printout model. Four different series of the tablets were manufactured (see ESI Figure S2 for images of printer preparation process and tablets recovery). As obtained tablets displayed significant porosity, they were stored in a desiccator at 20 % RH (relative humidity) and 22 ± 2 °C prior further analysis. Such storage conditions assured lack of structural and morphological changes of the printed tablets over a period of 36 months.

2.2.8.1 *Series A (Placebo)*: The powder bed (per 100 g) was composed of microcrystalline cellulose used as a filling and disintegrating agent and PVP used as a binder in 50/50 wt./wt. ratio.

2.2.8.2 *Series B (Quinapril hydrochloride 3 mg)*: Similarly to Series A, the powder bed (per 100 g) was composed of quinapril hydrochloride (2 g), microcrystalline cellulose (49 g) and PVP (49 g) (50/50 wt./wt. ratio). Both series (A and B) were designed as oblong tablets with the following dimensions: length 12.5 mm, width 5.5 mm, height 4.5 mm.

2.2.8.3 *Series C and D (Clotrimazole 40 and 50 mg)*: The powder bed was composed of CLO co-processed with PVP (50/50 wt./wt., see Section 2.2.6 for details) (28 g), microcrystalline cellulose (50 g) and PVP (50 g). The Series C tablets were design as oblong tablets with following dimensions: length 13.5 mm, width 9.5 mm, height 7.0 mm, while Series D tablets were 30 % longer (length 17.5 mm vs. 13.5 mm) to scale the dose of the tablet by 30%.

2.2.9 *Pharmaceutical parameters of the tablets*:

2.2.9.1 *Disintegration*: Disintegration time was determined for six tablets using ERWEKA ZT 51 disintegration tester (ERWEKA, Langen, Germany) according to European Pharmacopoeia. Briefly, the tablets were placed on a metal mesh in a plastic basket and each of the tablets was covered with a plastic ring to avoid flotation. The study was conducted in distilled water at 37 ± 0.5 °C. The disintegration time was measured for each tablet and given as an average \pm standard deviation.

2.2.9.2 *Friability*: To assess the tablets tendency to chip, crumble or break Electrolab EF friability tester (Electrolab India, Mumbai, India) was used. Five tablets were weighed, placed in the plastic drum, and revolved at 25 rpm for 4 minutes (100 rotations). The tablets were recovered from the plastic drum and their surface was brushed off dust prior weighting. The % loss of tablet mass after friability test was calculated using standard equation.

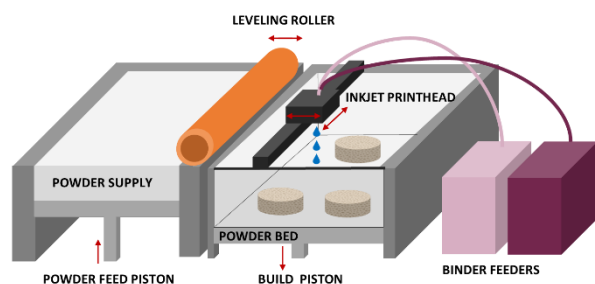
- 2.2.9.3 *Tablets hardness*: The crushing strength was measured for five tablets using MultiTest 50 (Dr. Schleuniger Pharmatron, Solothurn, Switzerland). Each tablet was placed in exact same position between the jaws of the instrument prior application of the stress. The measurements were repeated without proper cleaning of the surface of the jaws as prescribed by the European Pharmacopoeia.
- 2.2.9.4 *API content in the formulation*:
- 2.2.9.4.1 *Quinapril hydrochloride* [41,42]: The drug content was determined using ultra-high performance liquid chromatography (UHPLC, Thermo Scientific UltiMate 3000, Dionex Corporation, Sunnyvale, CA, USA) and LiChroCART® 125-3 Purospher® RP-18 (5 µm, Merck) column at 25 °C and the detector was set at the wavelength of 210 nm. The 55/45 V/V acetonitrile/water mobile phase at a flow rate of 0.9 mL/min was used in the analysis. Each of six tablets was placed in 50 mL volumetric flask and dissolved in phosphate buffer (pH = 6.8). 10 µL sample was injected on the column in triplicates.
- 2.2.9.4.2 *Clotrimazole* [43]: The drug content was determined using high performance liquid chromatography (HPLC, Agilent 1260 Infinity, Agilent Technologies, Waldbronn, Germany), Zorbax ODS C18 (5 µm, 4.6 x 150 mm, Agilent Technologies) column at 30 °C and the 70/30 V/V acetonitrile/water mobile phase at a flow rate of 1 mL/min. Each of six tablets was placed in 50 mL volumetric flask and dissolved in the 50/50 V/V mixture of water/methanol. 20 µL sample was injected on the column in triplicates.
- 2.2.9.5 *Drug dissolution study*: The dissolution studies were performed using USP type II apparatus Hanson SR-8 PLUS (Hanson, Chatsworth, CA, USA) in non-sink conditions. Each of the tablets were placed in the 150 mL vessel containing 100 mL of dissolution medium at 37 ± 0.5 °C and stirred at 100 rpm. The 3 mL samples were withdrawn through the in line 0.45 µm filters (Quality Lab Accessories LLC, Telford, PA, USA). To mimic pH of the oral cavity (pH = 6.7-7.3) [44] phosphate buffer (pH = 6.8) was used in the study of quinapril hydrochloride. The samples were withdrawn at 5, 10, 15, 30, 45, 60, 75 min with media replacement. In case of clotrimazole acetate buffer (pH = 4) was used to mimic vaginal pH (pH = 3.8-4.5) [45]. The samples were withdrawn at 5, 15, 30, 45, 60, 90, 120, 180 min with media replacement.
- 2.2.10 *Powder X-ray diffraction (PXRD)*: The phase of the APIs before and after 3D printing and spray drying processing was analysed using Bruker D2 PHASER diffractometer (Bruker AXS, Karlsruhe, Germany) using a LynxEye detector and Cu K α radiation (K α = 1.54184 Å). Bragg–Brentano ($\theta/2\theta$) horizontal geometry was used for data collection in the angular range between 3° and 36° 2 θ . A step size of 0.02° 2 θ and irradiation time of 1 s/step (neat reference substances and clotrimazole composites and tablets) or 4 s/step (quinapril hydrochloride tablets). The 2.5° Soller slit diffractometer optics was used with a divergence

slit of 0.2 mm, anti-air-scatter screen of 1 mm and Ni filter. The X-ray tube operated at 30 kV and 10 mA.

- 2.2.11 *Fourier-transform infrared spectroscopy (FTIR)*: FTIR spectra of API, pharmaceutical excipients and obtained tablets were acquired with Nicolet iS50 spectrometer (Thermo Scientific, Waltham, MA, USA) using an attenuated total reflectance (ATR) mode. The spectra were recorded over a wavelength of 400 cm^{-1} to 4000 cm^{-1} . Each spectrum was recorded using 32 scans at 4 cm^{-1} resolution. In case of quinapril hydrochloride tablets 128 scans were acquired.
- 2.2.12 *Differential scanning calorimetry (DSC)*: The DSC analysis was performed using DSC 214 Polyma (Netzsch, Selb, Germany) equipped with an IntraCooler. The materials samples (5-7 mg) were weighed to aluminium pans ($25\text{ }\mu\text{L}$) and sealed with pierced lids. The analysis was performed in the temperature range from 0 to $155\text{ }^{\circ}\text{C}$ in a nitrogen atmosphere (50 mL min^{-1}) using a heating rate of $5\text{ }^{\circ}\text{C min}^{-1}$. An empty pan sealed with a pierced lid was used as a reference. The DSC data analysis was performed using the Netzsch Proteus Analysis software 7.1.0 (16.10.2017). The instrument was calibrated using a set of six standards (6.239.2-91.3) supplied by Netzsch.
- 2.2.13 *Thermogravimetric analysis (TGA)*: The TG 209 F1 Libra Thermobalance (Netzsch, Selb, Germany) was used for the thermogravimetric analysis. The samples (7-10 mg) were placed in AL_2O_3 crucibles and heated from 25 to $800\text{ }^{\circ}\text{C}$ at $20\text{ }^{\circ}\text{C min}^{-1}$ in a protective atmosphere of dry nitrogen (50 mL min^{-1}). The obtained data were analysed using Netzsch Proteus Analysis software.

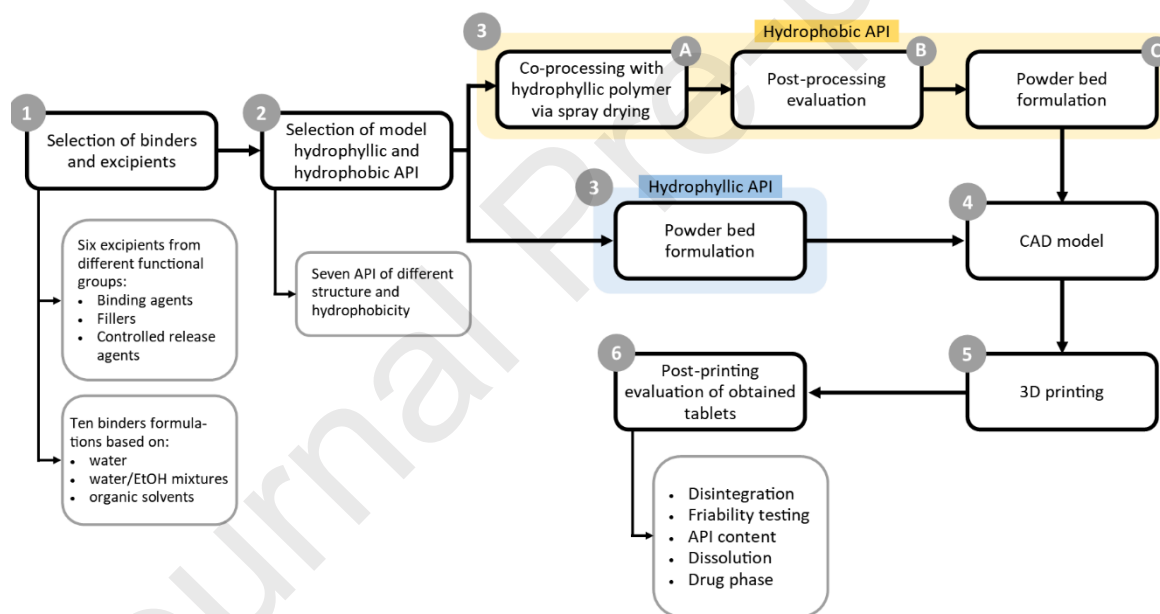
3. Results and Discussion

For successful formulation of the pharmaceutical tablets with specified properties (e.g., mechanical strength, short disintegration time, fast or modulated drug release) it is important to use pharmaceutically acceptable excipients of known quality enabling to control the properties of the final product. Furthermore, the selection of the formulation process (e.g., direct compression, granulation, hot melt extrusion or BJ) also limits the number of possible APIs or excipients which can be used in the formulation process. For example, thermolabile compounds have a limited application in hot melt extrusion, while APIs undergoing a phase change under high humidity conditions cannot simply be formulated using water-based granulation. In a similar way BJ is not a simple “plug and play” technique and, when applied to real life materials, it requires extensive optimisation (Scheme 1).



Scheme 1. Schematic representation of tablets printing using binder jetting technology (single column artwork, colour print).

Therefore, in this section we will provide a step-by-step optimisation process of both binder and powder bed composition considering materials properties relevant for BJ process e.g., powder wettability, powder permeability, gelation, binder viscosity and surface tension. This will be followed by the characterisation of BJ formulated pharmaceutical tablets composed of either freely soluble (quinapril hydrochloride) or practically insoluble (clotrimazole) APIs (Scheme 2).



Scheme 2. Flow chart of the work performed in this study using either hydrophilic (QHCl) or hydrophobic (CLO) drug model.

3.1 Binder (ink) and powder bed formulation

Although water is a solvent of choice in many pharmaceutical processes its high surface tension makes it difficult to apply in binder jetting technology of poorly wettable pharmaceuticals (both APIs and excipients). The poor selection of a binder and powder bed properties may result in sliding of powder layers during printing and a decrease of the final product quality (see ESI Figure S3). In this study seven

model APIs of different logP (see ESI Figure S4) and six excipients were selected to determine their wettability and permeability by water and formulated binders (Figure 1, ESI Table S1, Table S3).

3.1.1 Determination of powder wetting and permeation of binder through a powder bed

The contact angle measurements and powder bed permeability studies were firstly carried out for selected excipients as these are frequently used in a large excess as compared to an API in the solid dosage forms. Wettability of HPMC (of two different viscosities of 1% solutions in water referred here as 4000 cp and 100 000 cp), methylcellulose and ethylcellulose by water was poor (contact angle $99^\circ < \theta < 132^\circ$) as compared to PVP ($\theta = 33^\circ$) and microcrystalline cellulose which displayed complete wetting (contact angle $\theta = 0^\circ$). To improve wetting of the powders by the water-based binders both SLS and Tween 20 as surface-active agents as well as PVP (as a binder) were added. This resulted in a substantial decrease of the surface tension of obtained binders L1 and L2 to $40.7 \text{ mN} \cdot \text{m}^{-1}$ as compared to water (measured $71.0 \text{ mN} \cdot \text{m}^{-1}$; reference value $72.8 \text{ mN} \cdot \text{m}^{-1}$ at 20°C) and improvement of their wettability of selected excipients. The highest decrease of ca. 45° (from 132° to 87°) was observed for L2 binder in contact with ethylcellulose, while for other excipients a decrease of the measured contact angle value varied from 14° for HPMC 4000 cp (water $\theta = 99^\circ$ and binders L1 and L2 $\theta = 85^\circ$) to 36° for methylcellulose (water $\theta = 107^\circ$ and binder L2 $\theta = 71^\circ$) (Figure 1 and ESI Table S3).

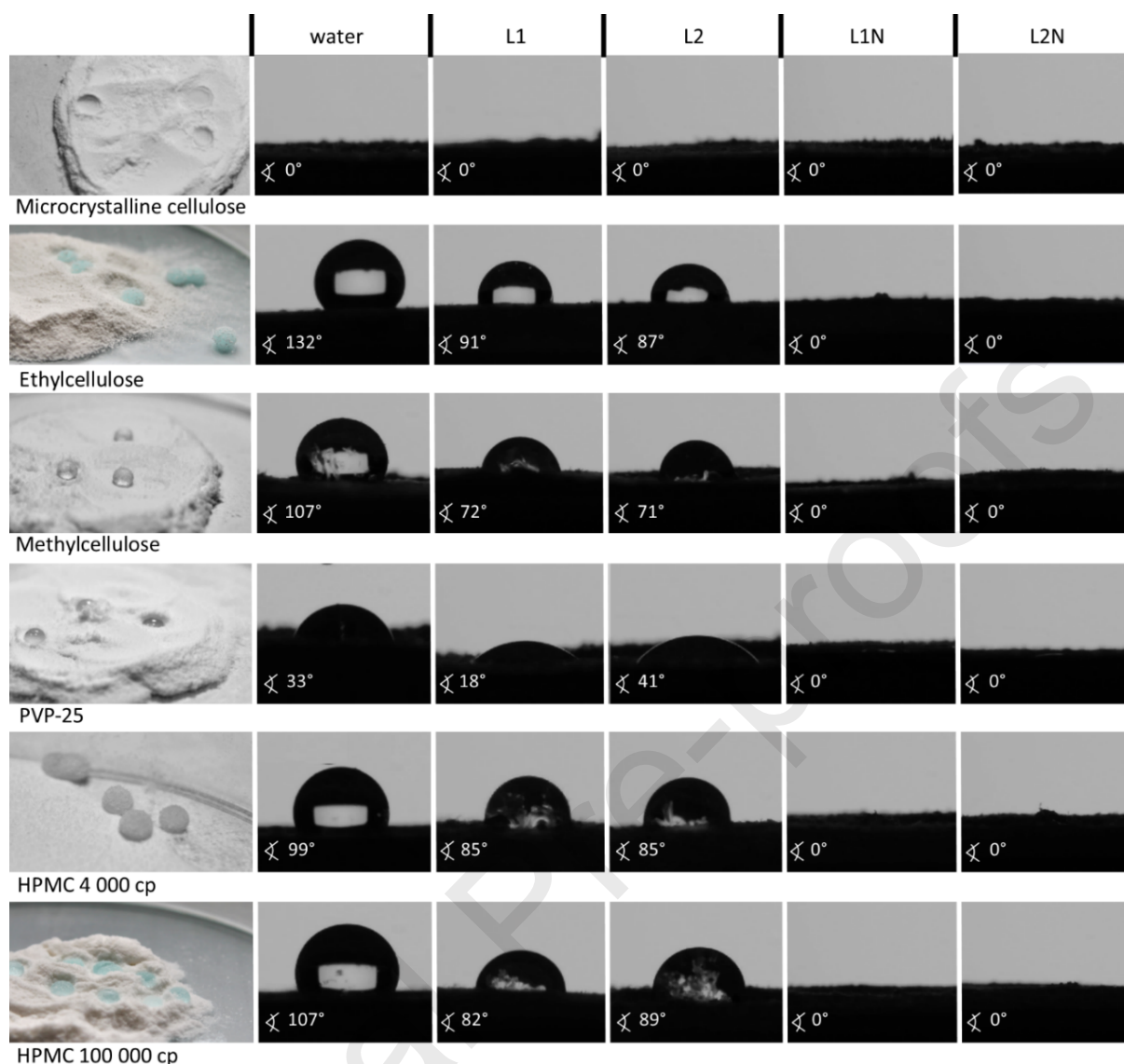


Figure 1. Powder bed permeability and contact angle values for selected excipients by water and selected binders. The blue colour of drops is due to the addition of methylene blue to the binder for better visualisation of the process (colour print).

As organic solvents have significantly lower surface tension compared to water, they can be considered for the use in formulation of binder solutions either alone or in a mixture with water. The evaluated water/ethanol mixtures (binders L1N and L2N) displayed a decrease of surface tension as compared to water and water-based binders (surface tension $30.9 \text{ mN} \cdot \text{m}^{-1}$) resulting in complete wetting of all selected excipients. Similarly, the wettability of selected excipients by binders formulated using organic solvents (Figure 1, ESI Tables S1 and S3) was significantly improved compared to water-based excipients. In most cases, almost complete wetting of the powder's surface was observed when using binders based on organic solvents (Figure 1, ESI Table S3). Similarly, differences were observed between wetting of selected APIs by water and formulated excipients. With decreasing logP of an API

the measured water contact angle decreased from 94° for clotrimazole ($\log P = 5.4$) to 0° for famotidine ($\log P = -0.6$) (see ESI Figure S4) which represents complete wetting.

While $\log P$ can be used as an indicator of good or poor water wettability of an API, it needs to be noticed that wettability of a solid is also related to its crystal structure (e.g. polymorphs, hydrates, cocrystals), crystal habit, orientation, and surface anisotropy [46–49]. The poor wetting of APIs by water-based binders could be overcome by the application of binders formulated using organic solvents and their mixtures with water. For example, near-complete wetting was observed for selected APIs using L1N binder composed of water/ethanol 50/50 V/V mixture (see ESI Figure S4).

Another important factor that needs to be considered during the selection of excipients and APIs is the permeability of the binder through a powder bed (Figure 1, Figure 2). The evaluation of binder permeability through the selected excipients and APIs indicated three types of behaviour: (i) restricted permeability due to low wettability (for APIs) and/or binder gelation in contact with polymer (HPMC, methyl- and ethylcellulose); (ii) powder bed dissolution and gelation upon contact with binder (PVP); and (iii) good permeability through the powder bed without gelation or powder dissolution (quinapril HCl and microcrystalline cellulose).

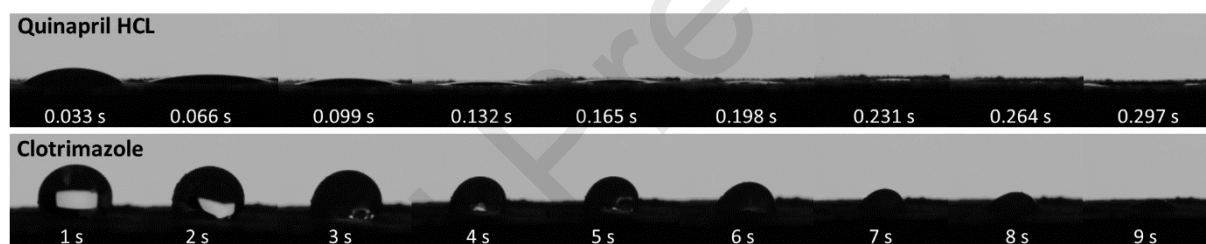


Figure 2. Permeability of water through the quinapril HCl and clotrimazole powder bed.

Based on the binder and powder bed optimisation process, binder L1N and the mixture of microcrystalline cellulose and PVP (50:50 wt. %) was selected as a base for inkjet printing of low dose tablets with hydrophilic quinapril HCl and hydrophobic clotrimazole as these two APIs displayed significantly different behaviour in contact with water and selected binders.

3.1.2 *Increasing powder wettability via spray drying co-processing of hydrophobic crystals with hydrophilic excipients*

As organic solvents in some cases may induce either phase change or dissolution of an API in the powder bed it is not always possible to use binders composed with organic solvents in inkjet 3DP process [22,23,50]. Therefore, we developed the approach of hydrophobic crystals co-processing with hydrophilic excipients using spray drying to increase the water wettability of poorly wettable clotrimazole used as a model drug (Figure 3A). In this method crystals of poorly soluble API are suspended in an aqueous solution of hydrophilic excipient (polymer or small molecule which undergoes amorphization during spray drying) and spray dried to obtain API crystals co-processed with molecules

that are wettable by water. We used PVP and lactose for CLO co-processing via spray drying due to their hydrophilic properties and wide use in tablet formulation.

Clotrimazole spray dried and co-processed with PVP or lactose does not undergo a polymorphic transformation, as evidenced from a PXRD patterns comparison of the obtained materials and the starting material CLO form I (Figure 3C and ESI Figure S5). With the increasing content of PVP or lactose in relation to the API in the obtained materials, a decrease in intensity of the CLO peaks as well as a slight elevation of the baseline, associated with an increased content of amorphous PVP or amorphous lactose is observed in the PXRD patterns. It is worth noting, that as a result of spray drying of lactose solutions, an amorphous powder is formed, which is a phenomenon widely described in the literature [51]. Clotrimazole form I melts at 143.1 °C (Figure 3B) [43,52]. The drug crystals co-processed with PVP showed a decrease of the melting point of CLO to ca. 131 °C for the 25:75 and 50:50 CLO:PVP formulations, as well as a significant broadening of the phase transition endotherm (Figure 3B). For the 75:25 CLO:PVP formulation, two overlapping melting peaks can be distinguished. The first broad endotherm starts at 128.2 °C, while the onset of a second peak is at ca. 137.9 °C.

The presence of two melting peaks in the DSC thermogram may indicate that there is a minimal content of polymer to be used to obtain uniform composites while the presence of two melting endotherms may indicate the presence of a mixture of co-processed and neat CLO crystals. This is corroborated with SEM images which displayed the presence of segregated CLO crystals next to CLO-PVP composites (see ESI Figure S10). FTIR spectroscopic analysis (Figure 3D) confirmed no changes in the molecular structure of CLO and excipients after their spray drying. Furthermore, with the increase of the content of individual components (PVP or CLO) in the formulations the increase of the intensity of the peaks characteristic for this component is observed. The following characteristic absorption bands can be distinguished in the CLO spectra: 3166 and 3063 cm^{-1} (aromatic C-H stretching), 1585, 1433 and 1305 cm^{-1} (C-C benzene ring stretching), 1210 cm^{-1} (C-N stretching), 1081 cm^{-1} (chlorobenzene), 904, 823, and 741 cm^{-1} (C-H stretching) [43,52,53].

The PVP characteristic absorption bands were observed at: 3450 cm^{-1} (OH stretching), 2928 cm^{-1} (CH stretching), 1655 cm^{-1} (C=O stretching of the carbonyl group), 1421 cm^{-1} and 1370 cm^{-1} (CH deformational modes of the CH_2 group), 1284 cm^{-1} (CN stretching) [54–56]. As amorphous lactose in contact with binders crystallized into monohydrate (see ESI Figure S5) the PVP co-processed CLO crystals were used in the formulation of 3D printed tablets. The structural characterization of lactose co-processed CLO crystals is described in ESI section S1, Figure S6 and large SEM images are given in ESI Figure S11.

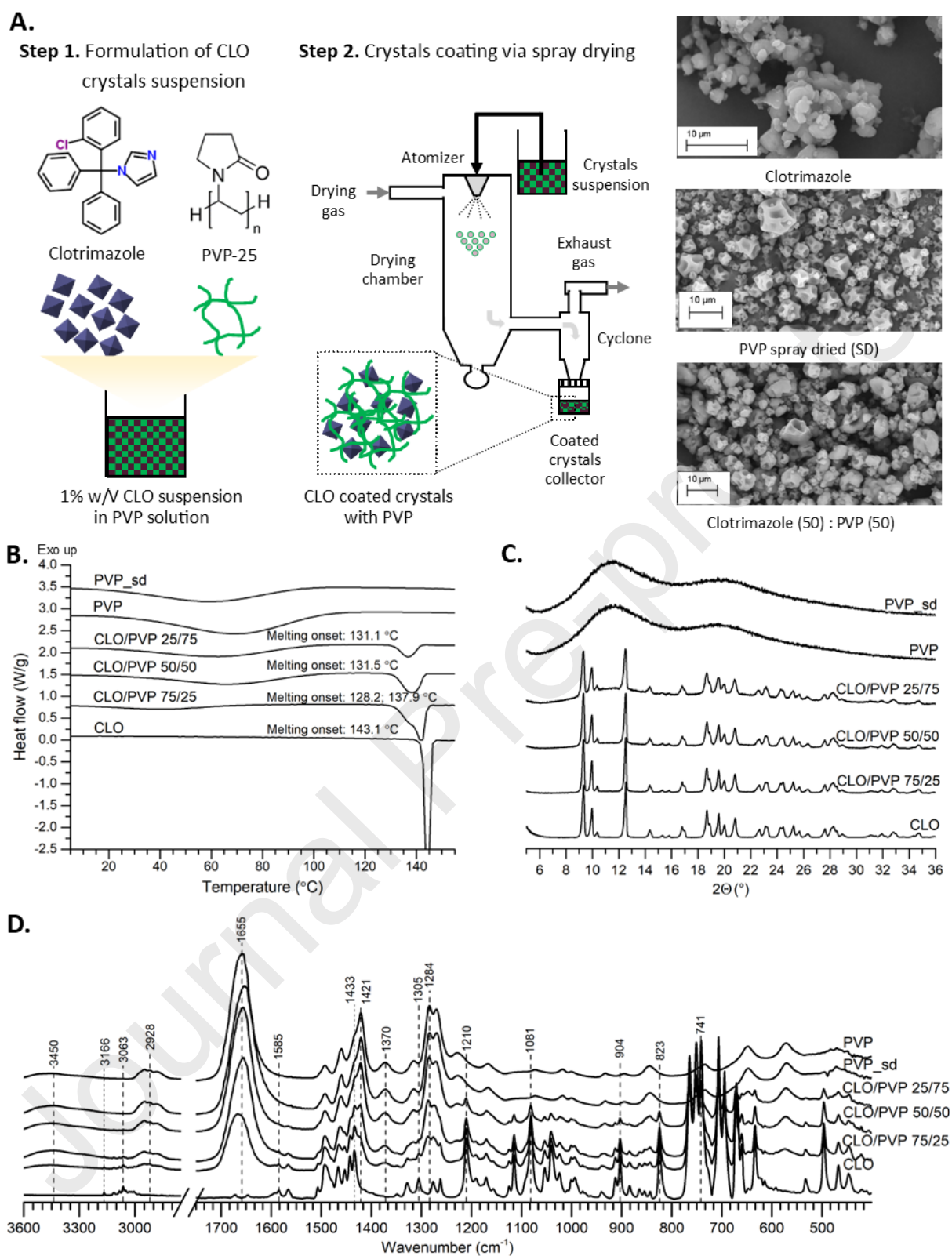


Figure 3. A. Schematic representation of crystal co-processing via spray drying method and SEM images of starting materials and obtained composites; B. DSC thermograms; C. PXRD patterns and D. FTIR spectra of CLO crystals co-processed with PVP at a different drug:polymer ratios. Large size SEM

images of starting materials along with co-processed CLO crystals are given in ESI Figure S10 (colour print).

As a result of spray drying, a significant improvement in the water wettability and permeability of CLO co-processed with both PVP and lactose was achieved (see ESI Figures S7 and S8). The spray drying processing of CLO crystals with PVP resulted in a decrease of water contact angle values from 94° for neat CLO to 46° for CLO:PVP 25:75 and 0° for CLO:PVP 50:50 materials. The co-processing of CLO with lactose resulted in near-complete wetting of the materials regardless of LAC content (see ESI Figure S7). Interestingly, the spray drying of CLO with Tween 20 alone resulted in a complete wetting of the powder by water and binders L1 and L1N. An increase in the contact angle values of PVP-CLO composites in contact with binders L1 and L1N compared to the neat API was observed. This could be due to the PVP-PVP interactions as both binders L1 and L1N are based on PVP solution. Despite increased contact angle PVP co-processed materials enabled quick permeation of binders L1 and L1N (see ESI Figure S8) and presented excellent binding properties of particles in contact with water and binders L1 and L1N after drying (see ESI Figure S9).

The efficiency of the spray drying process for the tested formulations was in the range from 68% for CLO suspension to 91% for the CLO:LAC 75:25 mixture (see ESI Table S2). The differences in the process efficiency were associated with properties of obtained materials i.e., a very fine, highly electrostatic powder was difficult to recover from the collector.

3.2 Inkjet-printed tablets: placebo (Series A), QHCl tablets (Series B) and CLO tablets (Series C and D)

To assess the feasibility of BJ 3D printing method to formulate tablets containing both hydrophilic (QHCl) and hydrophobic (CLO) APIs in the powder bed, four series of tablets were designed. Series A (placebo) contained only a mixture of MC and PVP without any API, Series B contained a low dose (3 mg) of the hydrophilic quinapril hydrochloride (QHCl) mixed with MC and PVP in the powder bed, while Series C and D contained hydrophobic CLO co-processed with PVP. To evaluate the dose scalability of the powder formulation, the dimension '1' (Figure 4A and D, see also Materials and methods Section 2.2.7) of Series C tablets were increased by 30% resulting in Series D.

3.2.1 Shape, size, mechanical properties and QHCl content in the tablets

Two series (A and B) of oblong tablets (Figure 4A and D) were prepared in accordance with the CAD design (Figure 4B). The tablets were printed using two designs without and with supporting printing platform to avoid initial powder layers shifting (Figure 4B and C). The size and shape of obtained tablets were in excellent agreement with designed values (see ESI Tables S4 and S5). Both series of tablets met the pharmacopeial criteria (Ph. Eur. 10th Edition) for mass uniformity with average masses determined as 126 ± 4.67 mg (Series A) and 149 ± 2.50 mg (Series B) (see ESI Tables S6 and S7). Furthermore,

obtained tablets displayed excellent resistance to mechanical stress with average crushing strength (see ESI Tables S8 and S9) of 45.5 ± 5.07 N (Series A) and 70.6 ± 15.42 N (Series B) and a mass loss of 1.18% (Series A) and 0.85% (Series B) after friability test. Short water disintegration time of both tablets 15 s (Series A) and 73 s (Series B), which may be related to their high porosity (see micro-CT analysis Figure 5 and SEM images Figure 6E) makes them suitable as orodispersible tablets (ODT). The QHCl content in Series B tablets was determined as 2.75 ± 0.039 mg, which is ca. 8% lower than designed dose of 3 mg (see ESI Table S10).

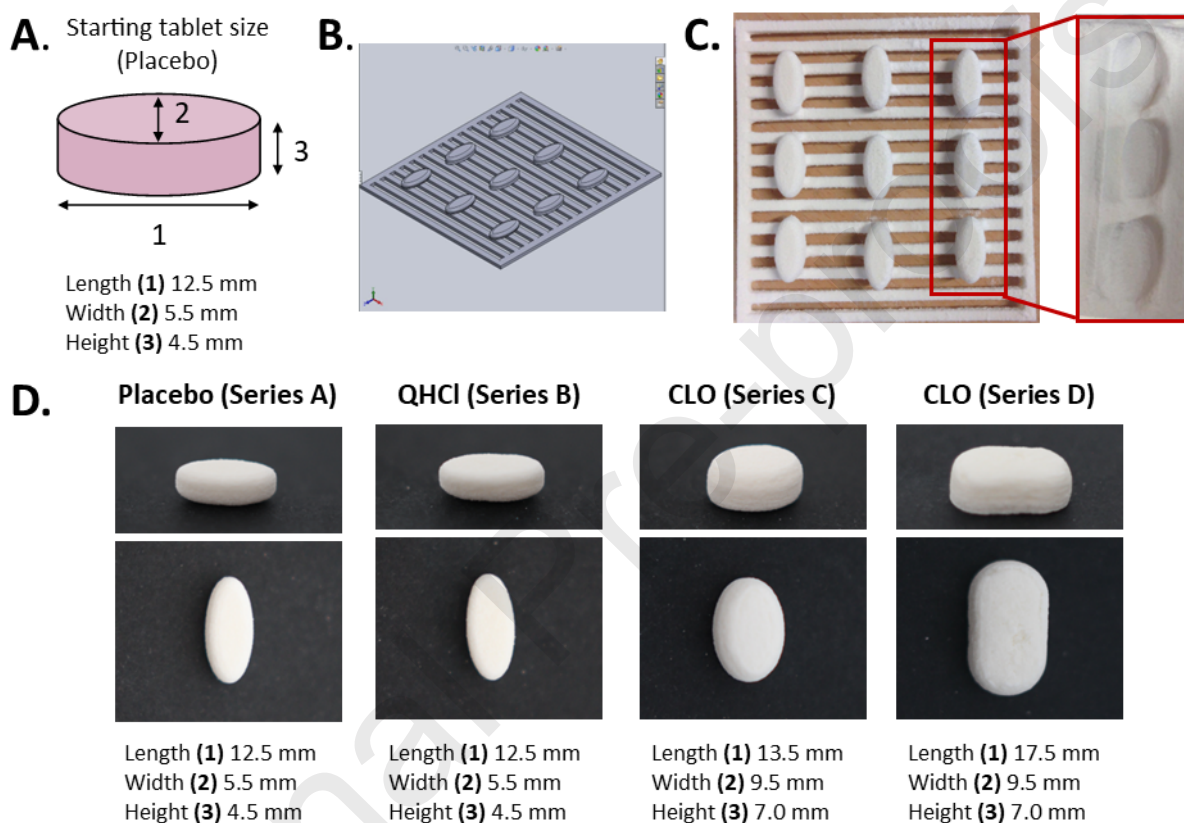


Figure 4. A. Size of the designed tablets (Series A and B); B. CAD design used for tablets printing; C. Printed placebo tablets on the supporting platform (inset shows printed tablets prior dusting); D. Representative images and dimensions of the obtained tablets (colour print).

3.2.2 Analysis of the microstructure of the tablets

The results of the examination in the form of 2D sections through the reconstructed tablets is shown in Figure 5. The microstructure of all tablets is similar and highly porous with many discontinuities visible in the analysed two-dimensional XCT sections (Figure 5A). To quantify the porosity present in the analysed tablets, an area of interest (ROI) with dimensions of 3 x 3 x 3 mm was selected from the centre of each tablet (Figure 5B). The XCT study allowed to identify two types of pores present in the tablets produced with the BJ technology i.e., open, and closed pores (Figure 5B). The registered total porosity for Series B tablets was 46%, while other three materials displayed slightly increased porosity of 54%

(Figure 5B). The open pores were predominately found within the tablets, which may explain short disintegration time of the obtained tablets. Closed pores were found in the range of 1-3 % of total porosity. Detailed analysis of the material porosity showed that the pores with the smallest diameters were the most abundant in the Series A tablets (Figure 5C), while both CLO tablets (Series C and D) had pores with largest diameters. These tablets were also characterized by the lowest sphericity (Figure 5C). The most spherical pores were recorded in the Placebo tablet.

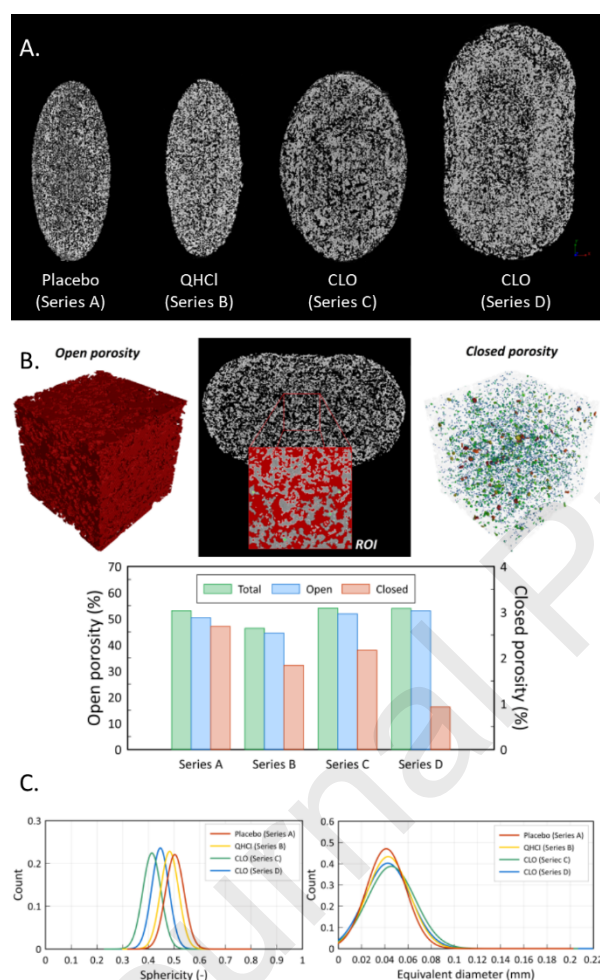


Figure 5. A. Two-dimensional XCT sections of Series A, B, C and D tablets; B. Porosity analysis of obtained tablets (Series D tablet with ROI and two types of porosity: open and closed inside it is given as an example); C. Sphericity (left) and equivalent diameters (right) of the pores formed within the obtained tablets (colour print, single column).

3.2.3 Structural properties of the QHCl incorporated in the tablets

Processing of the drug and excipients to form a 3D printed dosage form may affect the phase of an API (e.g. formation of hydrate/solvate or its amorphous state) leading to changes in drug dissolution and

bioavailability [23,26]. To assess the structure of QHCl incorporated in the powder bed we used state-of-the-art methods enabling to assess the phase of the drug incorporated in the tablets.

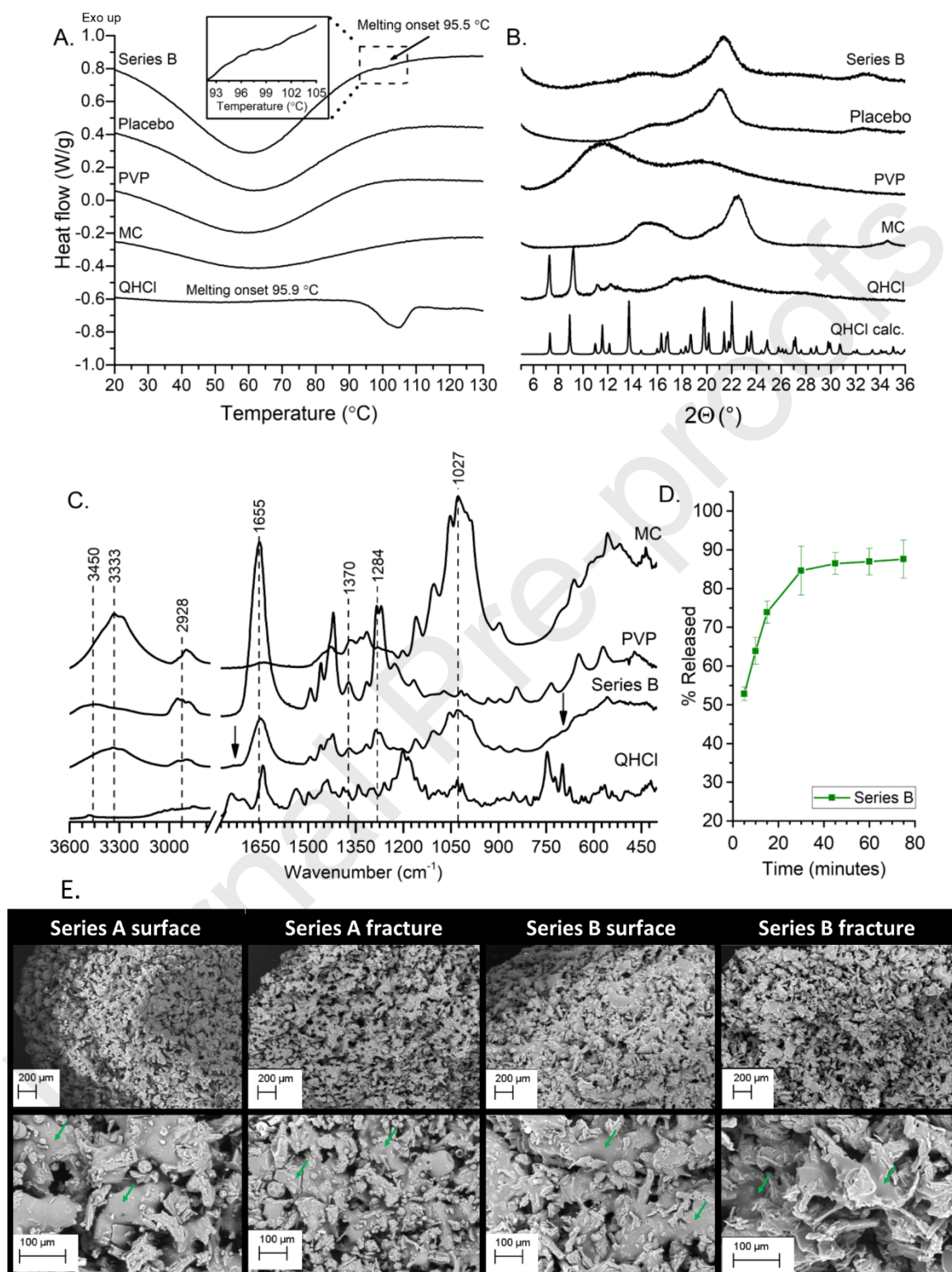


Figure 6. A. DSC thermograms; B. PXRD patterns and C. FTIR spectra of quinapril hydrochloride, microcrystalline cellulose, PVP, placebo tablets and Series B tablets. The inset in A. highlights melting of QHCl formulated as a 3DP tablet. The calculated PXRD patterns of QHCl (CSD ref. code SIWCEG

[57]) are given for comparison; D. Dissolution profile of QHCl 3DP tablets (Series B); E. SEM images of Series A and Series B tablets displaying porous structure of the tablet (see also ESI figure S12 and S13). Green arrows indicate polymer bridges formed after binder evaporation (colour print).

Quinapril hydrochloride forms crystals with a partial disorder as evidenced by the broad peaks appearing in the PXRD pattern above the angular value of $2\theta > 10^\circ$ and the broad melting endotherm of the API with the onset at 95.9°C (Figure 6A and B). DSC thermogram of the Series B tablets displayed the presence of a melting endotherm of quinapril hydrochloride at 95.5°C . The PXRD trace of Series B tablets is a superposition of amorphous 'halo' derived from PVP and MC. Lack of QHCl peaks in the diffractogram may be explained by the low content of the API in the obtained tablets (below 2% wt.) and the detection limit of the method (Figure 6B).

FTIR spectrum of Series B tablets (Figure 6C) displays characteristic vibrational bands of the tablets' components including MC at 3333 cm^{-1} (OH stretching), 2904 cm^{-1} (CH stretching), complex peak (in the range from $1164\text{--}1058\text{ cm}^{-1}$) with the maximum at 1027 cm^{-1} originating from the monosaccharide ring and PVP at 3450 cm^{-1} (OH stretching), 2928 cm^{-1} (CH stretching), 1655 cm^{-1} (C=O stretching of carbonyl groups), 1370 cm^{-1} (CH bending), 1284 cm^{-1} (CN stretching).

The presence of QHCl in the tablets is confirmed via small peaks observed as baseline elevation (marked with arrows in Figure 6C, Series B) at ca. 1740 cm^{-1} (stretching vibration of the carbonyl group in the carboxylic acid or ester) and 700 cm^{-1} (C-H out of plane bending from benzene ring). The dissolution analysis displayed the rapid QHCl release from the obtained tablets (Figure 6D). More than 50% of the dose was released after the first 5 minutes of the test while 80% of the dose was released within 30 minutes of the analysis. The fast release of the drug in the first few minutes of the test may be related to the short disintegration time (73 s) of the Series B tablets. The short disintegration time of the obtained tablets may be a consequence of their porous structure (See Section 3.2.2., Figure 5). SEM images revealed that drug, MC and solid PVP particles are loosely interconnected via PVP bridges, which are likely formed upon binder evaporation from the printed tablets (Figure 6E, green arrows).

3.3 Inkjet-printed tablets of CLO co-processed with PVP

3.3.1 Shape, size, mechanical properties, and drug content

The composition of powder bed and Series C tablets were designed to achieve the CLO dose of 45 mg in a single unit. The size of Series D tablets was further scaled to achieve a dose increase of ca. 30% as compared to Series C tablets by scaling dimension '1' by 33% (Figure 4D). The size and shape of obtained tablets were in excellent agreement with designed values (Figure 4D, ESI Tables S11 and S12). The mean mass of Series C tablets was $0.400\text{ g} \pm 0.014\text{ g}$, while mean mass of Series D tablets was $0.538\text{ g} \pm 0.026\text{ g}$. Both series of tablets met the Ph. Eur. requirements for the uniformity of the weight of tablets. The mechanical strength of obtained Series C and D tablets was increased as compared to placebo and QHCl tablets (Series A and B). The resistance to crushing of the Series C and D tablets

were 118.5 N and 151.8 N respectively (see ESI table S13). Furthermore, the obtained CLO tablets displayed significant abrasion resistance (the weight loss of Series C and D tablets after the friability test was 0.47%, and 0.70% respectively). The increased mechanical strength of the CLO tablets (Series C and D) as compared to Series A and B tablets may be a consequence of both increased size of the tablets as well as the co-processing the crystals crystal with PVP allowing for increased number of contacts between binding molecules (here PVP). SEM images of the obtained tablets displayed that the interconnecting PVP bridges are thicker as compared to Series A and B tablets and seem to form a continuous interconnected phase throughout the tablet (Figure 7E, ESI Figure S14). The surface of the tablets seems to be more rigid, while high porosity is still preserved (compare ESI Figure S14D-G surface and fracture of tablets). This, in turn, may result in increased mechanical strength of the tablets and ensure their short disintegration time of 55 and 84 s for Series C and D, respectively. The obtained Series C and D tablets contained $43.4 \text{ mg} \pm 5.1 \text{ mg}$ and $53.3 \text{ mg} \pm 5.7 \text{ mg}$ of CLO respectively (ESI Table S14), which agrees with the design dose of CLO in the formulations. It should be noted that larger tablets (Series D) were more difficult to print, and some of the printed objects had gaps between the powder layers.

3.3.2 *Structure and dissolution of the API incorporated in the tablets*

PXRD analysis confirmed the presence of form I of CLO in the obtained tablets of Series C and D (Figure 7B). This means that the incorporated drug did not undergo polymorphic transformation in contact with the binder solution. Similarly, the DSC thermogram of the Series C and D tablets showed melting endotherms of PVP co-processed CLO at 133.4 and 133.5 °C respectively (Figure 7A). The decrease of the melting onset of the CLO incorporated in the tablets as compared to neat CLO form I may indicate that the API crystals after the 3D printing process still contain PVP layer adsorbed on their surface. The almost identical heat of fusion of CLO recorded for both series of tablets proves the same concentration of API in the obtained tablets, which indicates the powder mixture does not segregate during printing.

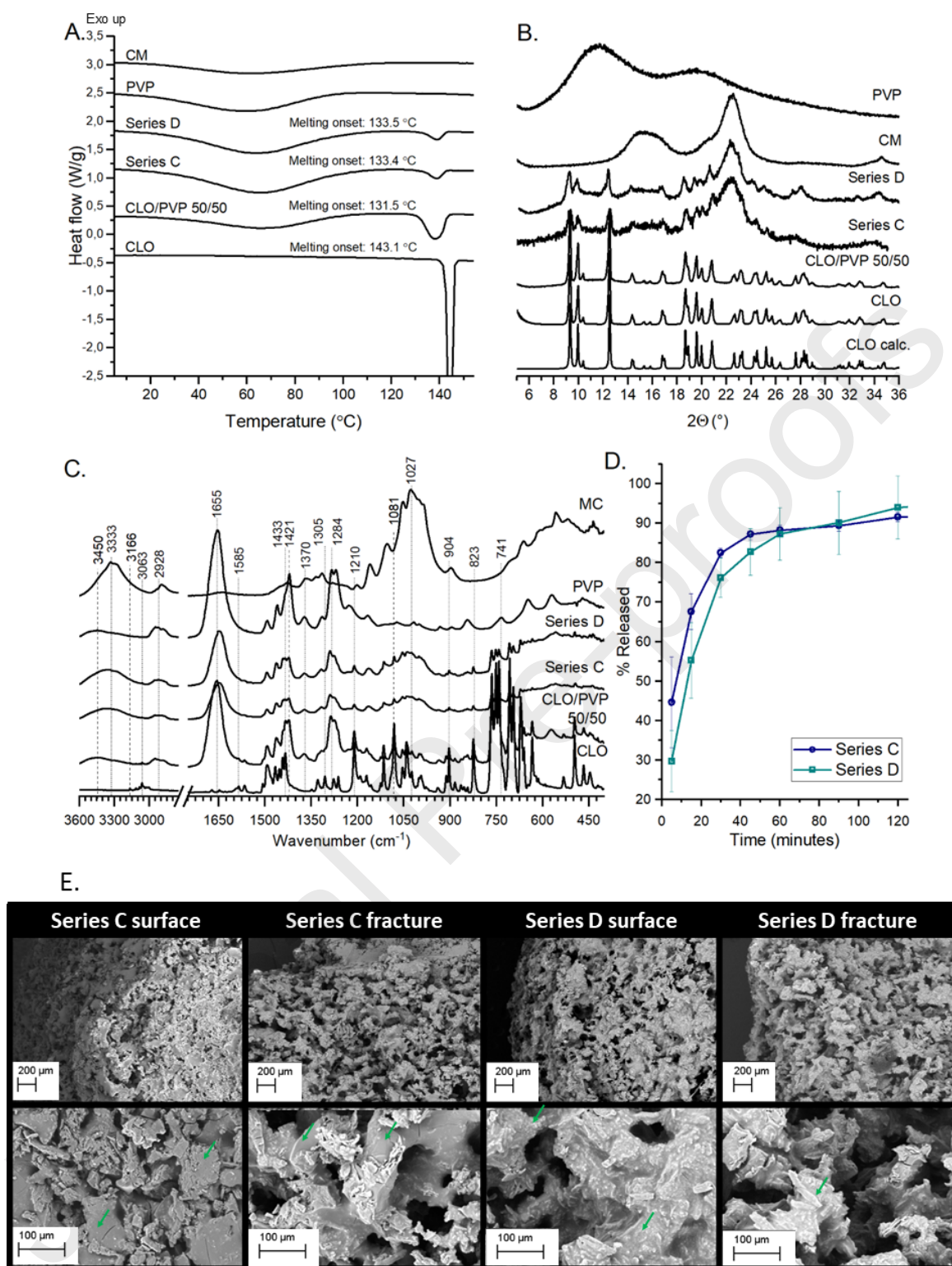


Figure 7. A. DSC thermograms; B. PXRD patterns and C FTIR spectra of clotrimazole (CLO), microcrystalline cellulose (CM), PVP, CLO/PVP 50/50 material, Series C and Series D tablets. The calculated PXRD patterns of CLO (CSD ref. code PUVRIH) are given for comparison; D. Dissolution profile of both CLO 3DP tablets (Series C and D); E. SEM images of Series C and Series D tablets displaying porous structure of the tablet (see ESI Figure S14). Green arrows indicate polymer bridges formed after binder evaporation (colour print).

The CLO form I structure incorporated in the tablets was also confirmed with FTIR (Figure 7C). The characteristic CLO bands were observed at 3166 and 3063 cm^{-1} (aromatic C-H stretching), 1585, 1433 and 1305 cm^{-1} (C-C benzene ring stretching), 1210 cm^{-1} (C-N stretching), 1081 cm^{-1} (chlorobenzene stretching), 904, 823, and 741 cm^{-1} (C-H stretching) [43,52]. The PVP characteristic absorption bands were observed at: 3450 cm^{-1} (OH stretching), 2928 cm^{-1} (CH stretching), 1655 cm^{-1} (C=O stretching of the carbonyl group), 1421 and 1370 cm^{-1} (CH deformational modes of the CH_2 group), 1284 cm^{-1} (CN stretching), while MC bands can be found as a complex peak (in the range from 1164-1058 cm^{-1}) with the maximum at 1027 cm^{-1} originating from the monosaccharide ring and at 3333 cm^{-1} (OH stretching) [55,56].

The CLO release from the obtained tablets was fast (Figure 7D). This is likely the consequence of highly porous microstructure of the tablets formed upon evaporation of binder (Figure 7E). For the Series C tablets, 80% of the dose was released within thirty minutes of the dissolution test, while nearly 50% of the dose was dissolved after 5 minutes of the test. The Series D tablets due to slower disintegration time and increased mechanical strength, released 30% of the dose within the first 5 minutes of the test while 80% of CLO was dissolved within 45 minutes of the test. The drug dissolution data indicates that the high porosity of the obtained tablets enables fast release of the incorporated API despite the limited volume of dissolution medium (i.e., 100 mL as compared to 900 mL in standard test), which may be used for the formulation of vaginal tablets.

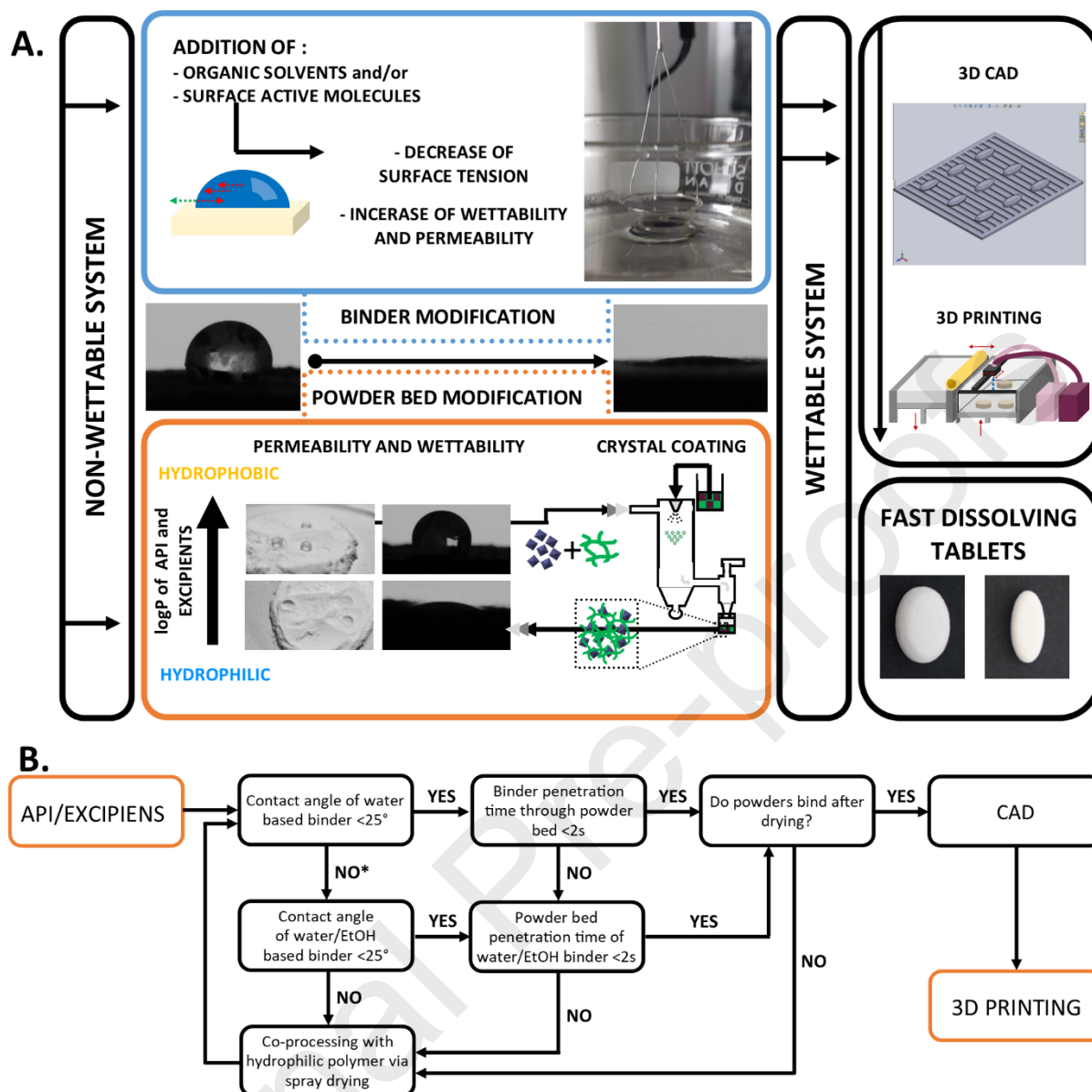
4. Summary and outlook

Additive manufacturing holds promise in the development of personalized drug delivery systems. These tailored materials are of importance for advanced treatment of clinically vulnerable individuals including elderly people with underlying diseases or children with clinical conditions requiring dose and/or administration route modifications. Binder jetting technology has advantage over other AM techniques as it enables to obtain robust pharmaceutical formulations using relatively simple mixtures of APIs and excipients bound together with binder solution.

4.1 Powder mixtures and modifications

In this work we presented formulation approach and powder mixture composition that allow formulating fast dissolving tablets with small dose (3 mg) of model hydrophilic API quinapril hydrochloride. Mixing QHCl with bulking (microcrystalline cellulose) and binding agent (PVP) enabled us to obtain porous fast dissolving tablets with satisfactory mechanical properties. As MC and PVP have excellent water wettability and permeability properties, these excipients may be considered as bulking and binding agents for other pharmaceutical formulations comprising hydrophilic APIs in small doses. Considering that both MC and PVP can be supplied from different manufacturers having variable particle sizes and morphologies, the assessment of permeability and spreadability of the binder through both materials and their mixture needs to be performed prior printing. This can simply be evaluated by dropping binder

solution on the test material and observing droplet behaviour upon contact with material (see Scheme 3A – Powder Bed Modification and 3B). If a drop quickly ($t < 2$ s) permeates through the powder it can be considered as good candidate for binder jetting. Furthermore, PVP (and other pharmaceutical polymers) can be supplied with different length of polymer chains (and other subtle structural changes) which in contact with water forms solutions of different viscosities. This can result in poor binder permeability as highly viscous liquid layer can be formed on the powder surface preventing permeation of a binder to distal powder layers and, consequently, compromising mechanical strength of the obtained tablets. Proposed formulation based on a mixture of MC and PVP may serve as a starting point for formulation of powder bed that comprise hydrophilic APIs; however, use of binder jetting for formulation of hydrophobic drugs pose a significant technological challenge. Even though diluting hydrophobic APIs with hydrophilic excipients can be used to improve permeability and wettability of powder composition by a binder solution, this strategy cannot be applied for large dose formulations.



*If after co-processing with hydrophilic polymer the materials are poorly wettable, a change of hydrophilic matrix is required.

Scheme 3. A. Binder and powder bed modification strategies enabling successful printing of hydrophobic APIs using binder jetting technology; **B.** Decision tree presentation for optimization process of binder and powder bed composition (colour print).

To enable processing hydrophobic APIs using binder jetting we developed a method of crystal co-processing with hydrophilic excipients via spray drying, which allows ‘hiding’ hydrophobic surface of the API crystals within hydrophilic matrix of excipient (e.g., PVP or lactose). In this method API is suspended in a water solution of hydrophilic excipient and subsequently spray dried to form a uniform drug polymer matrix. It needs to be noticed that API crystals can act as seeds for polymer solidification during spray drying and this process may form a basis to obtain homogenous composites. This approach was successfully used for formulation of fast dissolving clotrimazole tablets. Despite crystal co-

processing being an effective strategy allowing to overcome hydrophobicity limitations of the APIs used in binder jetting, it can be even more efficient when combined with modifications of binder solutions.

4.2 Binder modifications

In cases when it is not possible to modify the powder properties of API (e.g., by spray drying) changing composition of the binder may improve the printability of the powder mixture. In the optimization step described in this work we used water, water/ethanol mixture as well as several organic solvents (methanol, dichloromethane, acetonitrile, isopropanol) as basis for binder formulation. The use of low surface tension organic solvents (Scheme 3) mixed with binder (PVP) and surface-active agents (Tween 20, SLS) enabled to obtain binders with excellent wetting properties which may be applied for binder jetting printing of hydrophobic powders. As none of the evaluated solvents was fully compliant for the development of pharmaceutical formulations, we proposed the use of a binder based on water/ethanol mixture (50/50 V/V) with PVP and surface-active agents. The obtained binder had low surface tension ($\gamma = 30.9 \text{ mN} \cdot \text{m}^{-1}$) as compared with water ($\gamma = 71.0 \text{ mN} \cdot \text{m}^{-1}$) and water mixtures with PVP and surfactants ($\gamma = 40.7 \text{ mN} \cdot \text{m}^{-1}$). It needs to be highlighted that printing using water-based binders L1 and L2 (per nomenclature used in this work see ESI, Table S1) was not possible and resulted in powder layers shifting (this effect is shown in the Figure S3 in the ESI). This may indicate that the use of binders with surface tension below ca. $30 \text{ mN} \cdot \text{m}^{-1}$ may be required for printing hydrophobic pharmaceuticals using binder jetting technology. Therefore, the proposed binder LIN may be involved in binder jetting printing of pharmaceuticals due to its desirable rheological properties, low toxicity, and simple composition.

5. Conclusions

In this study we proposed a formulation approach for using binder jetting technology in the development of fast disintegrating, highly porous tablets with optimal mechanical strength and high pharmaceutical availability of API which contain either large doses of hydrophobic drug or small doses of hydrophilic API. The presented research has shown that a significant challenge in the development of solid dosage forms using BJ printing technology is the wettability of the powder bed. It was noticed that substances with a high partition coefficient (logP), characterized by poor wettability, are difficult to print using binder jetting. In this work, we presented the optimization protocol enabling the selection of ink with sufficient spreadability and permeability via evaluated pharmaceutical substances (APIs and excipients). A novel approach for the effective improvement of wettability of hydrophobic API via crystals co-processing with hydrophilic excipients using spray drying was presented for clotrimazole as a model drug. In this method crystals of hydrophobic APIs are spray dried with hydrophilic polymer or small molecules forming amorphous mass after spray drying which allows to hide hydrophobic surface of the crystals. Therefore, the increased wettability of the materials as well as increased mechanical strength of the tablets was observed. This could be explained by the homogenous distribution of the polymer on

the particle surface enabling a larger number of contacts between the binding molecules, either deposited at the surface of drug crystals or with the binding ink. Furthermore, as binder jetting technology can be used in the development of orodispersible paediatric formulations, we provide a robust printing protocol enabling us to manufacture highly uniform 3 mg quinapril tablets characterized by short disintegration time and excellent mechanical properties.

Acknowledgments

Authors would like to acknowledge the financial support from Ministry of Science and Higher Education via grant SUB.D190.20.004.

Author contributions

Conception, design and methodology: KPN, MR, P.S.-Z., BK; writing of the original draft of the manuscript: KPN, MK; manuscript review and editing: AMG, KM, MK, P.S.-Z., MR, BK, KPN; resources and methodology: KPN, MR, P.S.-Z., BK, AG; investigation: MK, AD, KPN, MR, AZ, AG, KM, P.S.-Z., G.Z.; analysis and interpretation of data: MK, AD, KPN.

Conflict of interest

No potential conflicts of interest were disclosed.

References:

- [1] D. Psimadas, P. Georgoulas, V. Valotassiou, G. Loudos, Three-Dimensional Printing in Pharmaceutics: Promises and Problems, *J. Pharm. Sci.* 101 (2012) 2271–2280. <https://doi.org/10.1002/jps>.
- [2] M. Araújo, L. Sa-Barreto, T. Gratieri, G. Gelfuso, M. Cunha-Filho, The Digital Pharmacies Era: How 3D Printing Technology Using Fused Deposition Modeling Can Become a Reality, *Pharmaceutics*. 11 (2019) 128. <https://doi.org/10.3390/pharmaceutics11030128>.
- [3] H. Öblom, E. Sjöholm, M. Rautamo, N. Sandler, Towards Printed Pediatric Medicines in Hospital Pharmacies: Comparison of 2D and 3D-Printed Orodispersible Warfarin Films with Conventional Oral Powders in Unit Dose Sachets, *Pharmaceutics*. 11 (2019) 334. <https://doi.org/10.3390/pharmaceutics11070334>.
- [4] N. Scoutaris, M.R. Alexander, P.R. Gellert, C.J. Roberts, Inkjet printing as a novel medicine formulation technique, *J. Control. Release*. 156 (2011) 179–185. <https://doi.org/10.1016/j.jconrel.2011.07.033>.

- [5] ZipDose Technology | Spritam | Aprecia, (n.d.). <https://www.aprecia.com/technology/zipdose> (accessed January 7, 2021).
- [6] A. Goyanes, A.B.M. Buanz, A.W. Basit, S. Gaisford, Fused-filament 3D printing (3DP) for fabrication of tablets, *Int. J. Pharm.* 476 (2014) 88–92. <https://doi.org/10.1016/j.ijpharm.2014.09.044>.
- [7] A. Goyanes, H. Chang, D. Sedough, G.B. Hatton, J. Wang, A. Buanz, S. Gaisford, A.W. Basit, Fabrication of controlled-release budesonide tablets via desktop (FDM) 3D printing, *Int. J. Pharm.* 496 (2015) 414–420. <https://doi.org/10.1016/j.ijpharm.2015.10.039>.
- [8] J. Wang, A. Goyanes, S. Gaisford, A.W. Basit, Stereolithographic (SLA) 3D printing of oral modified-release dosage forms, *Int. J. Pharm.* 503 (2016) 207–212. <https://doi.org/10.1016/j.ijpharm.2016.03.016>.
- [9] F. Fina, C.M. Madla, A. Goyanes, J. Zhang, S. Gaisford, A.W. Basit, Fabricating 3D printed orally disintegrating printlets using selective laser sintering, *Int. J. Pharm.* 541 (2018) 101–107. <https://doi.org/10.1016/j.ijpharm.2018.02.015>.
- [10] A. Awad, S.J. Trenfield, A. Goyanes, S. Gaisford, A.W. Basit, Reshaping drug development using 3D printing, *Drug Discov. Today*. 23 (2018) 1547–1555. <https://doi.org/10.1016/j.drudis.2018.05.025>.
- [11] H. Wickström, E. Hilgert, J. Nyman, D. Desai, D. Şen Karaman, T. de Beer, N. Sandler, J. Rosenholm, Inkjet Printing of Drug-Loaded Mesoporous Silica Nanoparticles—A Platform for Drug Development, *Molecules*. 22 (2017) 2020. <https://doi.org/10.3390/molecules22112020>.
- [12] E. Elele, Y. Shen, R. Boppana, A. Afolabi, E. Bilgili, B. Khusid, Electro-Hydrodynamic Drop-on-Demand Printing of Aqueous Suspensions of Drug Nanoparticles, *Pharmaceutics*. 12 (2020) 1034. <https://doi.org/10.3390/pharmaceutics12111034>.
- [13] S.A. Khaled, J.C. Burley, M.R. Alexander, C.J. Roberts, Desktop 3D printing of controlled release pharmaceutical bilayer tablets, *Int. J. Pharm.* 461 (2014) 105–111. <https://doi.org/10.1016/j.ijpharm.2013.11.021>.
- [14] A. Goyanes, P. Robles Martinez, A. Buanz, A.W. Basit, S. Gaisford, Effect of geometry on drug release from 3D printed tablets, *Int. J. Pharm.* 494 (2015) 657–663. <https://doi.org/10.1016/j.ijpharm.2015.04.069>.
- [15] M. Kyobula, A. Adedeji, M.R. Alexander, E. Saleh, R. Wildman, I. Ashcroft, P.R. Gellert, C.J. Roberts, 3D inkjet printing of tablets exploiting bespoke complex geometries for controlled and tuneable drug release, *J. Control. Release*. 261 (2017) 207–215. <https://doi.org/10.1016/j.jconrel.2017.06.025>.

- [16] S.A. Khaled, J.C. Burley, M.R. Alexander, J. Yang, C.J. Roberts, 3D printing of five-in-one dose combination polypill with defined immediate and sustained release profiles, *J. Control. Release.* 217 (2015) 308–314. <https://doi.org/10.1016/j.jconrel.2015.09.028>.
- [17] S.A. Khaled, J.C. Burley, M.R. Alexander, J. Yang, C.J. Roberts, 3D printing of tablets containing multiple drugs with defined release profiles, *Int. J. Pharm.* 494 (2015) 643–650. <https://doi.org/10.1016/j.ijpharm.2015.07.067>.
- [18] Y.J.N. Tan, W.P. Yong, J.S. Kochhar, J. Khanolkar, X. Yao, Y. Sun, C.K. Ao, S. Soh, On-demand fully customizable drug tablets via 3D printing technology for personalized medicine, *J. Control. Release.* 322 (2020) 42–52. <https://doi.org/10.1016/j.jconrel.2020.02.046>.
- [19] L.K. Prasad, H. Smyth, 3D Printing technologies for drug delivery: a review, *Drug Dev. Ind. Pharm.* 42 (2016) 1019–1031. <https://doi.org/10.3109/03639045.2015.1120743>.
- [20] C.J.H. Brenan, 3-D-Printed Pills: A New Age for Drug Delivery [From the Editor], *IEEE Pulse.* 6 (2015) 3–3. <https://doi.org/10.1109/MPUL.2015.2456651>.
- [21] D. Raijada, N. Genina, D. Fors, E. Wisaeus, J. Peltonen, J. Rantanen, N. Sandler, a step toward development of printable dosage forms for poorly soluble drugs, *J. Pharm. Sci.* 102 (2013) 3694–3704. <https://doi.org/10.1002/jps.23678>.
- [22] N. Genina, D. Fors, M. Palo, J. Peltonen, N. Sandler, Behavior of printable formulations of loperamide and caffeine on different substrates - Effect of print density in inkjet printing, *Int. J. Pharm.* 453 (2013) 488–497. <https://doi.org/10.1016/j.ijpharm.2013.06.003>.
- [23] G. Kollamaram, S.C. Hopkins, B.A. Glowacki, D.M. Croker, G.M. Walker, Inkjet printing of paracetamol and indomethacin using electromagnetic technology: Rheological compatibility and polymorphic selectivity, *Eur. J. Pharm. Sci.* 115 (2018) 248–257. <https://doi.org/10.1016/j.ejps.2018.01.036>.
- [24] N. Sandler, A. Määttänen, P. Ihalainen, L. Kronberg, A. Meierjohann, T. Viitala, J. Peltonen, Inkjet printing of drug substances and use of porous substrates-towards individualized dosing, *J. Pharm. Sci.* 100 (2011) 3386–3395. <https://doi.org/10.1002/jps.22526>.
- [25] W.S. Cheow, T.Y. Kiew, K. Hadinoto, Combining inkjet printing and amorphous nanonization to prepare personalized dosage forms of poorly-soluble drugs, *Eur. J. Pharm. Biopharm.* 96 (2015) 314–321. <https://doi.org/10.1016/j.ejpb.2015.08.012>.
- [26] H. Wickström, M. Palo, K. Rijckaert, R. Kolakovic, J.O. Nyman, A. Määttänen, P. Ihalainen, J. Peltonen, N. Genina, T. De Beer, K. Löbmann, T. Rades, N. Sandler, Improvement of dissolution rate of indomethacin by inkjet printing, *Eur. J. Pharm. Sci.* 75 (2015) 91–100. <https://doi.org/10.1016/j.ejps.2015.03.009>.

- [27] P.A. Meléndez, K.M. Kane, C.S. Ashvar, M. Albrecht, P.A. Smith, Thermal inkjet application in the preparation of oral dosage forms: Dispensing of prednisolone solutions and polymorphic characterization by solid-state spectroscopic techniques, *J. Pharm. Sci.* 97 (2008) 2619–2636. <https://doi.org/10.1002/jps.21189>.
- [28] L. Hirshfield, A. Giridhar, L.S. Taylor, M.T. Harris, G. V Reklaitis, Dropwise additive manufacturing of pharmaceutical products for solvent-based dosage forms, *J. Pharm. Sci.* 103 (2014) 496–506. <https://doi.org/10.1002/jps.23803>.
- [29] A.B.M. Buanz, M.H. Saunders, A.W. Basit, S. Gaisford, Preparation of personalized-dose salbutamol sulphate oral films with thermal ink-jet printing, *Pharm. Res.* 28 (2011) 2386–2392. <https://doi.org/10.1007/s11095-011-0450-5>.
- [30] K.J. Lee, A. Kang, J.J. Delfino, T.G. West, D. Chetty, D.C. Monkhouse, J. Yoo, Evaluation of Critical Formulation Factors in the Development of a Rapidly Dispersing Captopril Oral Dosage Form, *Drug Dev. Ind. Pharm.* 29 (2003) 967–979. <https://doi.org/10.1081/DDC-120025454>.
- [31] C.-C. Wang, M.R. Tejawani (Motwani), W.J. Roach, J.L. Kay, J. Yoo, H.L. Surprenant, D.C. Monkhouse, T.J. Pryor, Development of Near Zero-Order Release Dosage Forms Using Three-Dimensional Printing (3-DP™) Technology, *Drug Dev. Ind. Pharm.* 32 (2006) 367–376. <https://doi.org/10.1080/03639040500519300>.
- [32] D.G. Yu, C. Branford-White, Z.H. Ma, L.M. Zhu, X.Y. Li, X.L. Yang, Novel drug delivery devices for providing linear release profiles fabricated by 3DP, *Int. J. Pharm.* 370 (2009) 160–166. <https://doi.org/10.1016/j.ijpharm.2008.12.008>.
- [33] W.U. Weigang, Z. Qixin, G.U.O. Xiaodong, H. Weidong, The controlled-releasing drug implant based on the three dimensional printing technology: Fabrication and properties of, *J. Wuhan Univ. Technol. Mater. Sci. Ed.* 24 (2009) 977–981. <https://doi.org/10.1007/s11595-009-6977-1>.
- [34] K.P. O'Donnell, W.H.H. Woodward, Dielectric spectroscopy for the determination of the glass transition temperature of pharmaceutical solid dispersions, *Drug Dev. Ind. Pharm.* 41 (2015) 959–968. <https://doi.org/10.3109/03639045.2014.919314>.
- [35] U. Payumo, Francis C. (Somerville, MA, US), Sherwood, Jill K. (Edison, NJ, US), Monkhouse, Donald C. (Radnor, PA, US), Yoo, Jaedeok (West Orange, NJ, US), Gaylo, Christopher M. (Princeton Junction, NJ, US), Wang, Chen-chao (West Windsor, NJ, US), Cima, Micha, Method and form of a drug delivery device, such as encapsulating a toxic core within a non-toxic region in an oral dosage form, 7875290, 2011.

- [36] D. Psimadas, P. Georgoulas, V. Valotassiou, G. Loudos, Thermal Inkjet Application in the Preparation of Oral Dosage Forms: Dispensing of Prednisolone Solutions and Polymorphic Characterization by Solid-State Spectroscopic Techniques *PETER, J. Pharm. Sci.* 101 (2012) 2271–2280. <https://doi.org/10.1002/jps>.
- [37] D. Erdemir, V. Daftary, M. Lindrud, D. Buckley, G. Lane, A. Malsbury, J. Tao, N. Kopp, D.S. Hsieh, W. Nikitzuk, J.D. Engstrom, Design and Scale-up of a Co-processing Technology to Improve Powder Properties of Drug Substances, *Org. Process Res. Dev.* 23 (2019) 2685–2698. <https://doi.org/10.1021/acs.oprd.9b00354>.
- [38] V. Vanhoorne, E. Peeters, B. Van Snick, J.P. Remon, C. Vervaet, Crystal coating via spray drying to improve powder tabletability, *Eur. J. Pharm. Biopharm.* 88 (2014) 939–944. <https://doi.org/10.1016/j.ejpb.2014.10.018>.
- [39] L. Shi, C.C. Sun, Overcoming poor tabletability of pharmaceutical crystals by surface modification, *Pharm. Res.* 28 (2011) 3248–3255. <https://doi.org/10.1007/s11095-011-0518-2>.
- [40] H.M. Bay, K. Thomas, Systems and processes for spray drying hydrophobic drugs with hydrophilic excipients, (2000).
- [41] H. Kanchukommula, A.T. Subramaniam, J. Munusamy, K. Danapal, S. Sengodan, Method Development and Validation of Hydrochlorothiazide and Quinapril in bulk and tablet dosage form by RP-HPLC, *J. Pharm. Chem.* 1 (2014) 10. <https://doi.org/10.14805/jphchem.2014.art8>.
- [42] V.T. Gawande, P.B. Miniyar, Simultaneous Estimation of Quinapril Hydrochloride and Hydrochlorothiazide from Pharmaceutical Formulation by Using UV, IR and RP-HPLC Anti-hyperlipidemic and Hypoglycemic agents View project, *Artic. Asian J. Chem.* 26 (2014) 3799–3804. <https://doi.org/10.14233/ajchem.2014.15935>.
- [43] B. Karolewicz, M. Gajda, A. Owczarek, J. Pluta, A. Górniak, Physicochemical characterization and dissolution studies of solid dispersions of clotrimazole with pluronic F127, *Trop. J. Pharm. Res.* 13 (2014) 1225–1232. <https://doi.org/10.4314/tjpr.v13i8.5>.
- [44] S. Baliga, S. Muglikar, R. Kale, Salivary pH: A diagnostic biomarker, *J. Indian Soc. Periodontol.* 17 (2013) 461–465. <https://doi.org/10.4103/0972-124X.118317>.
- [45] P.G. Larsson, J.J. Platz-Christensen, The vaginal pH and leucocyte/epithelial cell ratio vary during normal menstrual cycles, *Eur. J. Obstet. Gynecol. Reprod. Biol.* 38 (1991) 39–41. [https://doi.org/10.1016/0028-2243\(91\)90205-Y](https://doi.org/10.1016/0028-2243(91)90205-Y).
- [46] V. Puri, A.K. Dantuluri, M. Kumar, N. Karar, A.K. Bansal, Wettability and surface chemistry of crystalline and amorphous forms of a poorly water soluble drug, *Eur. J. Pharm. Sci.* 40 (2010) 84–93. <https://doi.org/10.1016/j.ejps.2010.03.003>.

- [47] C.A. Prestidge, G. Tsatouhas, Wettability studies of morphine sulfate powders, *Int. J. Pharm.* 198 (2000) 201–212. [https://doi.org/10.1016/S0378-5173\(00\)00341-0](https://doi.org/10.1016/S0378-5173(00)00341-0).
- [48] J.Y.Y. Heng, A. Bismarck, A.F. Lee, K. Wilson, D.R. Williams, Anisotropic surface energetics and wettability of macroscopic form I paracetamol crystals, *Langmuir*. 22 (2006) 2760–2769. <https://doi.org/10.1021/la0532407>.
- [49] S.R. Modi, A.K.R. Dantuluri, S.R. Perumalla, C.C. Sun, A.K. Bansal, Effect of crystal habit on intrinsic dissolution behavior of celecoxib due to differential wettability, *Cryst. Growth Des.* 14 (2014) 5283–5292. <https://doi.org/10.1021/cg501084a>.
- [50] N. Genina, E.M. Janßen, A. Breitenbach, J. Breitzkreutz, N. Sandler, Evaluation of different substrates for inkjet printing of rasagiline mesylate, *Eur. J. Pharm. Biopharm.* 85 (2013) 1075–1083. <https://doi.org/10.1016/j.ejpb.2013.03.017>.
- [51] J. Hellrup, M. Holmboe, K.P. Nartowski, Y.Z. Khimyak, D. Mahlin, Structure and Mobility of Lactose in Lactose/Sodium Montmorillonite Nanocomposites, *Langmuir*. 32 (2016) 13214–13225. <https://doi.org/10.1021/acs.langmuir.6b01967>.
- [52] S. Mittapalli, M.K.C. Mannava, U.B.R. Khandavilli, S. Allu, A. Nangia, Soluble Salts and Cocrystals of Clotrimazole, *Cryst. Growth Des.* 15 (2015) 2493–2504. <https://doi.org/10.1021/acs.cgd.5b00268>.
- [53] G.P. Sheeja Mol, D. Aruldas, I. Hubert Joe, S. Balachandran, A. Ronaldo Anuf, J. George, A.G. Nadh, Structural activity, fungicidal activity and molecular dynamics simulation of certain triphenyl methyl imidazole derivatives by experimental and computational spectroscopic techniques, *Spectrochim. Acta - Part A Mol. Biomol. Spectrosc.* 212 (2019) 105–120. <https://doi.org/10.1016/j.saa.2018.12.047>.
- [54] S. Sethia, E. Squillante, Solid dispersion of carbamazepine in PVP K30 by conventional solvent evaporation and supercritical methods, *Int. J. Pharm.* 272 (2004) 1–10. <https://doi.org/10.1016/j.ijpharm.2003.11.025>.
- [55] I.A. Safo, M. Werheid, C. Dosche, M. Oezaslan, The role of polyvinylpyrrolidone (PVP) as a capping and structure-directing agent in the formation of Pt nanocubes, *Nanoscale Adv.* 1 (2019) 3095–3106. <https://doi.org/10.1039/c9na00186g>.
- [56] H.M. Zidan, E.M. Abdelrazek, A.M. Abdelghany, A.E. Tarabiah, Characterization and some physical studies of PVA/PVP filled with MWCNTs, *J. Mater. Res. Technol.* 8 (2019) 904–913. <https://doi.org/10.1016/j.jmrt.2018.04.023>.
- [57] R.J. Hausin, P.W. Coddling, Molecular and Crystal Structures of MDL27,467A Hydrochloride and Quinapril Hydrochloride, Two Ester Derivatives of Potent Angiotensin Converting

Journal Pre-proofs